Advanced laboratory techniques: gamma emission in the decay of ^{226}Ra

Helena Massana Cid
*Facultat de Física, Universitat de Barcelona, Diagonal 645, 08028 Barcelona, Spain.**

Abstract: This work deals with the measurement of the gamma radiation emitted in the decay chain of ^{226}Ra. A theoretical study was carried out to give an approximation of the probabilities and polartity of the transitions. An inside on gamma interactions with matter helped to understand the observed spectrum. The final measurement, done with a scintillator, was analized and compared with previous studies on this matter. The discrepancies observed were justified by the low resolution of the used detector.

I. INTRODUCTION

The purpose of this work was to measure the gamma radiation emerging from the decay of ^{226}Ra. This radionuclide is the most common isotope of Radium and leads to a decay chain including beta and alpha decays followed by gamma decays. Alpha and beta decays will often lead to excited states of the daughter nucleus, causing gamma emission. The present study focused on these gamma transitions. The energy involved in this process is low, therefore the treatment was non-relativistic.

A theoretical framework is provided in section II, wich is used for a later discussion on the probability and types of transitions. Section III shows the decay chain of ^{226}Ra. The next section gives an inside on gamma spectroscopy, *i.e.* describing the materials and methodologies used in this type of experiments and concretely on the measurement performed. The results are exposed on the final section and they are compared with the values given in the literature [1, 2]. The intensities of the peaks are justified using the theoretical background given in section II. Finally the quality of the results is discussed and the conclusions are formulated.

II. INTERACTION OF ELECTROMAGNETIC RADIATION WITH ATOMS

In this section the probability and the selection rules for gamma transitions will be found. For that it is of need to know how the atom interacts with an electromagnetic field. The total Hamiltonian for a system formed of an atom and an external electromagnetic field characterized by the four-potential $A^\mu = (\Phi, \vec{A})$ is $H = H_{pauli} + H_{field}$[1][3]. It is useful to write it as $H = H_0 + H'$ where $H_0 = H_{atom} + H_{field}$ [2] and H' is the part that induces transitions between H_0 states. In the Coulomb gauge[3] H' can be written as:

$$H' = \frac{e^2}{mc}\vec{p}\cdot\vec{A} + \frac{e^2}{mc^2}A^2 + \frac{e\hbar}{2mc}\sigma\cdot(\vec{\nabla}\times\vec{A}) \qquad (1)$$

These three terms are defined as H_1, H_2 and H_m, respectively. H_2 is proportional to A^2, that means it describes the processes involving two fotons. H_2 can be neglected, as well as H_m [4]. The states of the system can be written as $|\Psi\rangle = |\Psi_{atom}\rangle\,|\Psi_{field}\rangle = |\Phi\rangle\,|...n_\lambda...\rangle$[4]. From the Fermi's Golden Rule [4] it is known that the probability of transition between an initial state $|\Psi_i\rangle$ and a final state $|\Psi_f\rangle$ is given by:

$$T_{i\to f} = \frac{2\pi}{\hbar}|M_{fi}|^2\rho(E_f) \qquad (2)$$

Where $\rho(E_f)$ is the density of final states and, in the first order of the perturbation theory, $M_{fi} = \langle\Psi_f|\,H'\,|\Psi_i\rangle$.

The vector potencial can be expressed as a function of the creation and annihilation operators as:

$$\vec{A}(\vec{r}) = \sum\nolimits_\lambda C(\omega_\lambda)(b_\lambda e^{i\vec{k_\lambda}\cdot\vec{r}} + b_\lambda^\dagger e^{-i\vec{k_\lambda}\cdot\vec{r}})\hat{\epsilon}_\lambda \qquad (3)$$

Where $\hat{\epsilon}_\lambda$ is the polarization direction of the field and $C(\omega_\lambda) = \sqrt{2\pi\hbar c^2/L^3\omega_\lambda}$.

In this study the importance relies on the emission of photons. In this case $|\Psi_i\rangle = |\Phi_i\rangle\,|...0_\lambda...\rangle$ and $|\Psi_f\rangle = |\Phi_f\rangle\,|...1_\lambda...\rangle$. Knowing how the creation and annihilation operators work, the commutation rules between $\vec{p}$ and $\vec{r}$, and using the conservation of energy [5] $E_i - E_f = \hbar\omega_\lambda$ it is easy to conclude that:

$$M_{fi} = \sqrt{\frac{2\pi\hbar e^2\omega_\lambda}{L^3}}\hat{\epsilon}_\lambda\cdot\left\langle re^{-i\vec{k}\cdot\vec{r}}\right\rangle \qquad (4)$$

Since the wavelenght of the photons is much larger than the size of the nucleus, the approximation $e^{-i\vec{k}\cdot\vec{r}} \sim 1$ can be done. From the series expansion of the exponential[6] this is a *dipole* (L=1). Then, the transition rate[7], replacing the density for its value and integrating over all possible direction of emission [4], is:

$$\lambda(E1) \equiv T^{E1}_{i\to f} = \frac{4e^2\omega_\lambda^4}{3c^3}\,|\langle r\rangle|^2 \approx \frac{e^2E^3}{(\hbar c)^4}r_0^2A^{2/3} \approx 1,0\cdot10^{11}A^{2/3}E[keV]^3 \qquad (5)$$

---

* helena.massanacid@gmail.com

[1] The Pauli hamiltonian H_{pauli} is a nonrelativistic hamiltonian for particles of spin 1/2 interacting with an electromagnetic field.

[2] $H_{atom} = \sum_i p_i^2/2m + V$; $H_{rad} = \sum_\lambda \hbar\omega_\lambda b_\lambda^\dagger b_\lambda$ where V includes all the interactions within the atom and $b_\lambda^\dagger$ and b_λ are the creation and annihilation operators for bosons.

[3] $\nabla^2\varphi = -4\pi\rho$; $\vec{\nabla}\cdot\vec{A} = 0$, which implies $\vec{p}\cdot\vec{A} = \vec{A}\cdot\vec{p}$.

[4] Using the occupation number formalism.

[5] Since the mass M of the nucleus is big ($\Delta E >> Mc^2$) then $\Delta E \simeq E_\gamma$. The energy recoiled by the nucleus is negligible.

[6] $e^{-i\vec{k}\cdot\vec{r}} = \sum_l(-i\vec{k}\cdot\vec{r})^l/l! = \sum_l(-ikr\cos\theta)^l/l!$.
It can be identified as the classical electromagnetic multipoles of order l.

[7] Probability per unit time for photon emission, in s^{-1}.

In equation (5) the radial parts of the nuclear wave functions are assumed to be constant up to the nuclear radius R [8][5]. The same can be done for $L > 1$ [4]. For example:

$$\lambda(E2) \approx 1,0 \cdot 10^4 A^{4/3} E[keV]^5 \tag{6}$$

There can also be magnetic transitions, where the radial term is r^{L-1}. The final expressions for the two first magnetic multipoles are [4]:

$$\begin{aligned} \lambda(M1) &\approx 5,6 \cdot 10^9 E[keV]^3 \\ \lambda(M2) &\approx 3,5 \cdot 10^4 A^{2/3} E[keV]^5 \end{aligned} \tag{7}$$

These are the Weisskopf estimates. They are not accurate computations and only give good relative comparisons between the probabilities of transitions. Usually, the lowest multipole predominates and the electric multipoles have a higher transition rate than magnetic multipoles [4]. However, not all of them are always allowed. In the emission of the photon two quantities must be conserved: the angular momentum and the parity. Therefore, a certain rules must be fulfilled *(Selection rules)*. These are [5]:

$$\begin{aligned} &|J_i - J_f| \leq L \leq J_i + J_f \text{ (no L=0)} \\ &\text{EL: } \pi_i \pi_f = (-1)^L \text{ ; ML: } \pi_i \pi_f = (-1)^{L+1} \end{aligned} \tag{8}$$

Where L is the angular momentum of the photon emitted, J_i and J_f are the angular momentum of the initial and final state of the atom, respectively, and $\Delta\pi$ is the change of the parity.

III. THE DECAY CHAIN OF ^{226}Ra

A sample of ^{226}Ra was measured. This element is unstable, and leads to a series of decays, like alpha and beta decays. ^{226}Ra has a half-life of 1600 years. Subsequent atoms in the chain are usually not in the ground state. This excited states decay via gamma radiation into a lower state, until they reach the ground state. In this text the alpha and beta decays are not discussed. The different probabilities (intensities) to reach each state can be found in the literature [6]. Sometimes the same element can decay into two different isotopes via alpha decay or via beta decay. Figure 1 shows[9] the decay chain of ^{226}Ra [6].

IV. GAMMA SPECTROSCOPY

There are two basic types of detectors used in gamma spectroscopy: scintillators (e.g. NaI detectors) and semiconductor detectors (e.g. Germanium detectors). The detector used in this study was a NaI detector.

A. Experimental assembly

The experimental assembly used is shown in Figure 2, which is the usual assembly needed when scintillators are used.

[8] $R = r_0 A^{1/3}$, with $r_0 \simeq 1,2$ fm and A the atomic mass number.
[9] There is also a small possibility (10^{-9}%) that ^{210}Pb leads to a parallel decay chain which ends at ^{206}Pb.

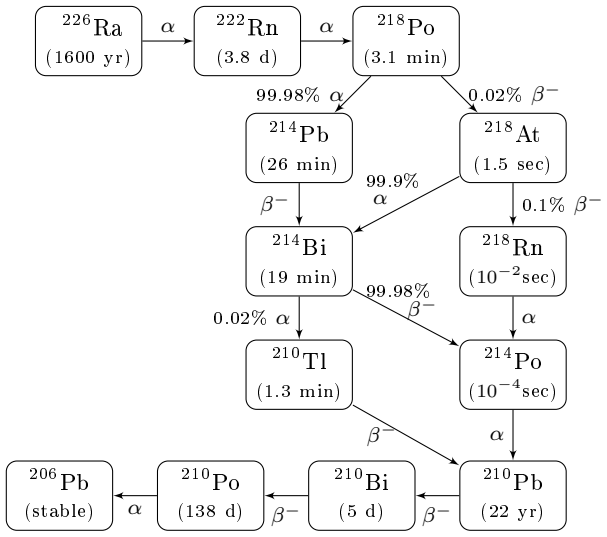

FIGURE 1: Decay chain of ^{226}Ra.

The process from the entrance of the gamma ray until the result is seen on the PC screen is the following. First a photon coming from the sample enters the detector, which is surrounded by lead to avoid the background radiation and where several interactions, discussed in the next section, may occur. These interactions lead to the arrival of photons in the optical range to the photocathode, in which, due to photoelectric effect, the photons excite electrons, setting them free from their atoms. The photoelectrons reach the photomultiplier tube (PMT). The PMT is connected to a High Voltage (HV) source and is linear only in a certain range of voltage and signal. Inside this tube there are dynodes. When an electron hits one of them it pulls out more electrons. In the end, after the electron has passed several dynodes, typically $10^4 - 10^6$ electrons for each photoelectron arrive at the anode. Once the electrons pass the anode, the electric charge is turned into a proportional voltage pulse. After this, in the Multichannel Analyzer (MCA), also called Pulse High Analyzer (PHA) the signal is turned into a digital and visual representation of the counts *versus* the channel number, which corresponds to the height of the pulse measured. Counts can be seen as the number of photons of that energy that have arrived. A calibration can be done with isotopes that emit photons of known energy to obtain a relationship Channel-Energy and obtain the calibrated spectrum.

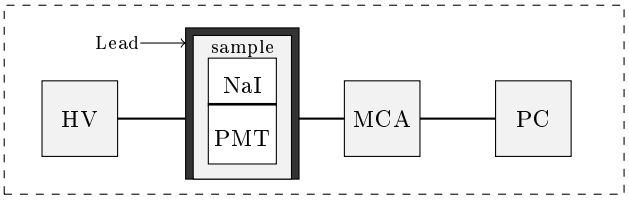

FIGURE 2: Experiment assembly. See abbreviations in the text.

The statistical error in gamma-ray spectrometry follows a Poisson distribution. Then, the relative statistical error is:

$$\epsilon_{stat.} = \sigma/N = [\sqrt{N}]^{-1} \quad (9)$$

Where σ is the standard deviation of the Poisson distribution, which is equal to the square root of the mean count rate N (property of this distribution).

The detector has a certain energy resolution, which depends on the energy and which can also depend on the high voltage. For each full energy peak one the resolution is defined as [7]:

$$R = \Delta E(fwhm)/E \quad (10)$$

Where $\Delta E(fwhm)$ is the full width at half maximum of the peak.

B. Gamma interactions with the detector

Gamma interactions with matter are relevant for the detector response function [7]. When a bunch of photons enter the detector, different things can happen: some of the photons pass right through it, not leaving any trace; some of them do not deposit all their energy due to interactions with the detector and a fraction of them deposit all the energy leading to the photopeak (also called full energy peak). Each peak will have a certain width due to statistical variations.

One of three main interactions is the photoelectric effect: the photon excites an atomic electron, the resulting free electron excites the atoms or molecules coming in his way until it loses all its energy and it is reabsorbed. These atoms emit photons of lower energy than the one that entered the scintillator. The photons arrive to the photocathode initiating the process descrived above.

The photon can be scattered and it leaves the detector. The deposited energy[10] is emited by the excited atoms and affects the spectrum from very low energies to the Compton edge, slightly below the photopeak. This is the Compton plateau. There can also be a energy peak around 200 keV, which is caused by photons that are backscattered in the lead that surrounds the detector and return to be absorbed[11].

Pair production can also occur if the energy of the photon is high enough ($E_\gamma \geq 1022$ keV). The photon annihilates into an e^- and a e^+. Then, the electron ionizes the atoms in the same way as the electron in the photoelectric effect. The positron, when it has low enough energy, annihilates with an atomic electron into two photons. If one of these scapes it leads to a peak of energy $E_\gamma - 511$ keV, if the two scape the peak is at $E_\gamma - 1022$ keV. If none of them scape the contribution goes to the full energy peak.

[10] When the initial energy of the photon is E_γ and it comes out with an angle θ, the final energy of the photon is $E'_\gamma = E_\gamma/\left[(1 + E_\gamma/mc^2)(1 - \cos\theta)\right]$, and the atom is left with an extra energy $\Delta E = E_\gamma - E'_\gamma$

[11] The exact position depends on the energy of the photon (E). If $E >> m_e c^2$ then $E' \sim m_e c^2/2 = 250keV$.

The probability of all these interactions is given by the cross section, which depends on the energy and the material.

V. EXPERIMENTAL RESULTS AND DISCUSSION

A. Calibration and background radiation

First of all a calibration to determine the relationship Channel-Energy and also to check if the PMT is linear at 750 V was done. The known peaks of ^{137}Cs (661.6 keV), ^{60}Co (1173.2 keV and 1332.5 keV) and ^{22}Na (1274,5 keV and 511.0 keV) were used [8–10]. The result obtained doing a lineal fit [11] to the measurements taken during 900 seconds (a good amount of time to minimize statistical error) gave the relationship Channel-Energy with a correlation coeficient of $R^2 = 0.999884$, proving to be linear.

Also the background radiation[12] was measured. The results were: Background= 5.6 counts/s ; Signal with Ra =259.3 counts/s. The absolute effect of the background was smaller than the statistical error of the signal. Therefore the effect of the background was neglected.

B. Peak mesurment

A measurement was taken during 2.5 days and the peaks were identified [1, 2]. Equation (9) indicates that the relative statistical error associated with these measurement is of 0.01%. Figure 3 shows the spectrum, already calibrated, in log scale to better appreciate the low intensity peaks. The observed peaks are shown in the Table I.

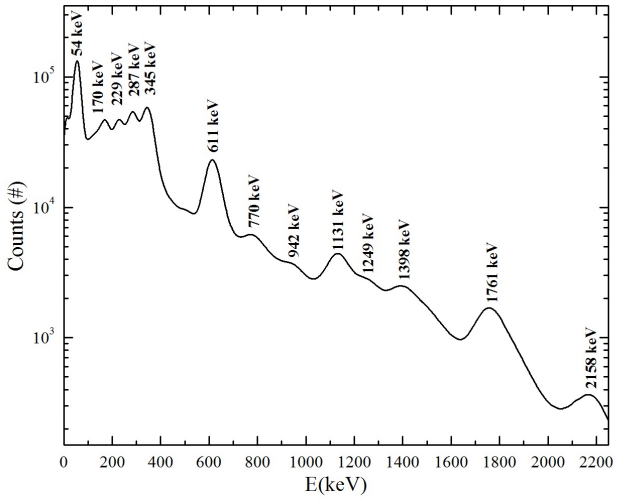

FIGURE 3: Gamma spectrum of ^{226}Ra

The intensities were measured computing the area under the peak and subtracting the continuous below it [11]. The intensity of the 611 keV peak is taken as reference to express the other intensities ($I_{m,611} \equiv 100$).

[12] The background radiation is the radiation occurring from other things than the sample, *e.g.* cosmic radiation.

E_m	I_m	R	E_t	I_m/I_t	J_i^π	J_f^π	EL,ML	λ_{ML}	λ_{EL}
54	254.8	0.57	-	-	-	-	-	-	
170	18.4	0.18	186	2.15	2^+	0^+	E2	-	0.30
229	13.3	0.12	242	0.82	1^-	2^-	M1,E2	0.01	1.06
287	22.7	0.09	295	0.55	1^-	1^-	M1,E2	0.01	2.86
345	36.4	0.10	352	0.45	1^-	1^-	M1,E2	0.02	6.92
611	100.0	0.11	609	-	2^+	0^+	E2	-	107
770	6.0	0.09	768	0.56	2^+	2^+	M1,E2	0.25	342
942	1.1	0.06	934	0.16	2^+	2^+	M1,E2	0.46	910
1131	10.3	0.07	1120	0.31	2^+	2^+	M1,E2	0.79	2256
1249	0.3	0.03	1238	0.02	2^+	2^+	M1,E2	1.06	3722
1398	6.3	0.07	1378	0.72	2^+	0^+	E2	-	6360
			1408	1.16	1^-	2^+	E2	-	7083
1761	12.6	0.08	1765	0.36	1^+	0^+	M1	3.08	-
2158	1.0	0.05	2119	0.09	1^+	0^+	M1	5.33	-
			2204	0.39	1^+	0^+	M1	6.00	-

TABLE I: Peaks observed in the gamma spectrum shown in Fig. 3. Label meaning and units in the text.

In Table I E_m and E_t are the measured and the reference energy in keV [1, 2], respectively, R is the resolution computed with equation (10), I_m/I_t is the quotient between the measured and the reference intensities [2], J_i^π and J_f^π are the initial and final angular momentum and parity of the atom, EL/ML is the possible polarity of the radiation acording to the selection rules of equation (8) and λ is the transition rate in $10^{19}s^{-1}$ to the lowest multipoles computed acording to equations (5), (6) and (7).

Two of the peaks shown in Table I (1298 keV and 2158 keV) could be supepositions of two of the peaks found in the literature. Both are indicated.

An intense peak was seen at 54 keV, which was probably coming from K emission lines of the surrounding lead. These emission lines are known to be 75 keV and 73 keV [12], which are not exactly our measured value. However, we have to keep in mind that at these low energy our system may not be completely linear. In fact, there is a transition that emits a photon of 53 keV, but it is of very low intensity (i.e. 2.49 according to [2]) compared with the one measured .

Every full energy peak has his compton plateu at lower energies, which explains the decreasing continuum below the peaks, besides the fact that for high energies the probability of interaction (cross section) is small [13]. At first look no scape peak could be observed. The resolution was better (diminished) when the energy increased.

Figures 4 and 5 show the gamma decay schemes for the transitions measured with the relevant transitions that can contribute to these. Above each energy level the momentum and parity J^π (left) and the energy in keV (right) is shown. In the right side of the levels the beta decay intensities are indicated. The gamma transition in

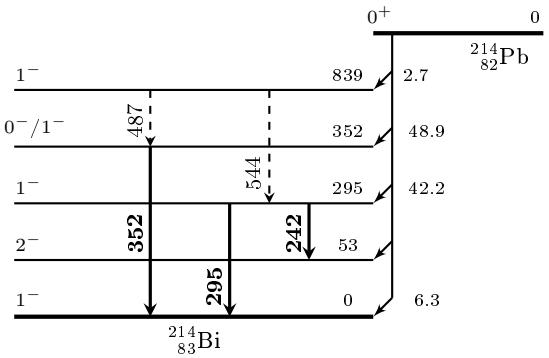

FIGURE 4: β decay of $^{214}_{82}$Pb showing the observed gamma transitions and the most relevant contributing.

^{222}Rn that leads to a peak of 186 keV it is not drawn since the main contribution to the 170 keV peak was the backscattering peak, as explained ahead.

In Figure 5 the dashed arrows stand for several transitions coming from several levels. The one in the left represents 7 transitions and the one in the right 5 transitions. They are not drawn for sake of simplicity. There are also two extra transitions that end in levels 2017 and 1764, but they are of very low intensity. Also, there is another transition that emits a photon of 609 keV (coming from ^{218}Rn $\rightarrow$ ^{214}Po), but is of much lower intensity that the one in the Figure 5.

A representation was done for E_m *vs.* E_t, and a linear fit was adjusted. The result was $E_t = 0,983E_m + 14,379$, with $R^2 = 0,9997$. Therefore, the relationship is linear as expected, but with a deviation in the origin ordinate.

A discussion on the intensities and the probabilities of transition was done from two perspectives. On the one hand, the experimental values obtained were compared with other experimental values from the literature obtained with higher resolution detectors as Germanium detectors [2]. On the other hand, the experimental values were compared with the transition rate probabilities shown in equations (5), (6), (7).

Table I shows that the measured and the reference intensities differed, *i.e.* $I_m/I_t \neq 1$. The only case that $I_m > I_t$ was for the 170 keV peak, because of the main contribution of the backscattering peak. Besides from this case, the intensities measured were lower than the intensities given in the literature, which can be explained by the finite size of the detector. As explained above, some photons with high energies can pass right through the detector without being detected, since higher the energy smaller the cross section [13], *i.e.* lower probability of interaction. In the very wide peaks the difficulty regarding its measurement can be a cause of the discrepancy.

Moreover, the general divergence in the intensity values probably comes from the low resolution of the NaI detector compared to the ones used in the literature, causing a superposition of the peaks and thus difficulting the subtraction of the continuum.

The intensities were also compared with the decay

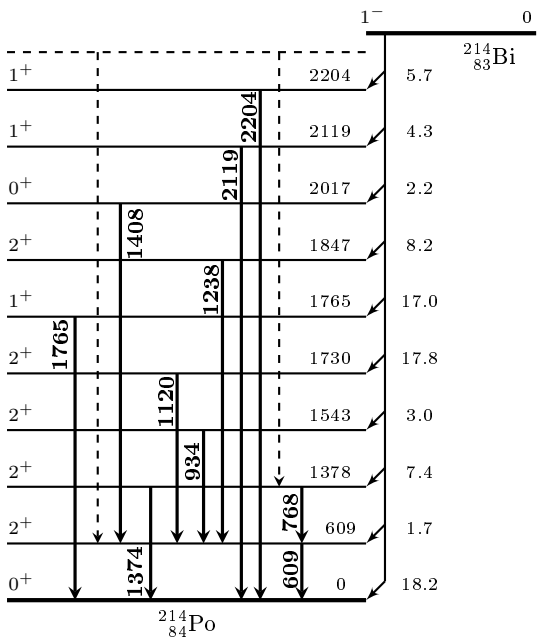

FIGURE 5: β decay of $^{214}_{82}$Pb showing the observed gamma transitions and the most relevant contributing.

rates λ. It has to be taken into account that the population of each initial level is also relevant, which depends on the probability of decay (beta or alpha) into that state and on the other gamma transitions that populate that state, shown in Figures 4 and 5. This is not reflected when λ is computed.

Several transitions are discussed next, starting with the three transitions in ^{214}Bi. Figure 4 shows that the probability of beta decay into the initial states is similar for all of them, and that there is one other transition which populates each initial state. Therefore, the intensity difference should be explained with the decay rate, which is shown in Table I that was increasingly higher for the three transitions, as well as the intensity. Therefore, in this case the results suited the Weisskopf estimates. However, for the transitions in ^{214}Po the more intense peak was not the one with higher decay rate, but on the contrary. That is understood looking at Figure 5 in which a lot of transitions end in the 609 keV level.

A similar justification could be done for the intensity of rest of the transitions.

VI. CONCLUSIONS

Gamma radiation can give us an idea of the energy, angular momentum and parity of the excited states of atoms by measuring the properties of the emitted photons. The intensity and the energy of several transitions were measured with a scintillator, compared with theoretical approximations and with the references in the literature. The energies measured were pretty accurate and the Weisskopf estimates gave an idea of the probability of the transitions. However, the intensities measured did not match the results found in the literature. That is mainly because the available detector used for this study did not have enough resolution, making it harder to subtract the continuum below the peaks and to differentiate them. One way to perform the same study in a more accurate manner would be to use a Germanium detector for example, which has typically a resolution of one order of magnitude better than scintillators. Doing this, not only the intensity measurments would be better but also the identification of additional peaks would be enabled.

VII. ACKNOWLEDGMENTS

The author gratefully acknowledges the support of the tutor and advisor Prof. Ricardo Graciani, without which the present study could not have been completed. The author would like to convey thanks to Prof. José María Fernández Varea for his advice and to the University for providing the laboratory facilities. Last but not least, I also thank all friends and family who have helped and supported me.

[1] S. C. Wu. "Nuclear Data Sheets". Vol. 110:681-748 (2009).
[2] D. Sardari, T. D. MacMahon. "Gamma-Ray Emission Probabilities in the Decay of ^{226}Ra and Its Daughters". Journal of Radioanalytical and Nuclear Chemistry, Vol. 244: 463-469 (2000).
[3] M. Weissbluth, *Atoms and Molecules* (Academic Press, New York, 1978).
[4] MIT OpenCourseWare: Applied Nuclear Physics `http://ocw.mit.edu/courses/nuclear-engineering/22-02-introduction-to-applied-nuclear-physics-spring-2012/lecture-notes/MIT22_02S12_lec_ch7.pdf` Accessed 8 June 2014.
[5] K.S. Krane, *Introductory Nuclear Physics* (John Wiley & Sons, New York, 1988).
[6] M.M. Bé, V. Chisté, C. Dulieu. "Le Radium 226 et ses descendants". Note techique LNHB/04-04 (2004).
[7] University of Florida: Gamma Ray Spectroscopy `http://www.phys.ufl.edu/courses/phy4803L/group_I/gamma_spec/gamspec.pdf`. Accessed 8 June 2014.
[8] E. Browne, J. K. Tuli. "Nuclear Data Sheets". Vol. 108: 2173-2318 (2007).
[9] J. K. Tuli. "Nuclear Data Sheets" Vol. 100: 347–481 (2003).
[10] R.B. Firestone. "Nuclear Data Sheets" Vol. 106: 1–88 (2005).
[11] Origin (OriginLab, Northampton, MA)
[12] Harvard Medical School: X-Ray Emission Lines `http://www.med.harvard.edu/jpnm/physics/refs/xrayemis.html` Accessed 8 June 2014.
[13] R.L. Heath. "Scintillation Spectrometry: Gamma ray spectrum catalogue" Idaho Falls, Idaho, U.S. Atomic Energy Commission, Idaho Operations Office. Vol. 1 (1964)